

Characterization and Correction of Artifacts from Dynamic Interaction between Motion and Position Dependent Off-Resonance Patterns

K. K. Pandey¹, and D. Noll¹

¹Biomedical Engineering, University of Michigan, Ann Arbor, MI, United States

Introduction: The net effect of motion on fMRI is due to many artifact generating mechanisms. Physical movement of the brain in the scanner can cause false activations [1] and image registration can introduce interpolation errors [2,3]. Movement during fMRI scan reorients the interface between air cavities and brain tissue both of which have different susceptibilities. This can cause dynamic variations in off-resonance patterns throughout the brain and, as a result, dynamically changing artifacts. Such dynamic artifacts reduce the accuracy of image registration. Further, even after “perfect” image registration, they introduce variability in the time-series thus reducing sensitivity of functional contrast.

In this study, we characterized the position dependent off-resonance artifacts in a susceptibility phantom and, investigated the effectiveness of image reconstruction methods for spiral fMRI that do off-resonance correction using different types of fieldmaps. In particular, we evaluated Conjugate Phase (CP) gridding reconstruction [4] with - static and motion corrected fieldmaps; and a model based iterative image reconstruction with - static, motion corrected, and jointly estimated dynamic fieldmaps [5,6].

We found that iterative reconstruction with dynamically updated fieldmaps was best able to compensate for orientation dependent dynamic off-resonance artifacts followed by iterative and CP gridding reconstruction methods that use fieldmaps motion corrected with respect to static fieldmaps. The commonly used static fieldmap based off-resonance correction was least effective. This trend was also reflected in the effectiveness of motion correction of images reconstructed using the above listed methods and off-resonance correction measures.

Methods: A small metal pin was attached to the inferior surface of a spherical silicon phantom to emulate the field distortions in the human head. Axial images were acquired using a 3T GE scanner with, TE=25msec, TR=5s, FOV=22cm, size [64x64] and a combined reverse & forward spiral GRE sequence. The phantom was imaged at four orientations. Between each orientation, the phantom was rotated by 4 deg in coronal plane and a translated by 1mm in the z-direction. Four shot, high resolution images and fieldmaps, size [256 x 256] were acquired at each location and motion parameters were estimated with FLIRT [7] using these images.

Fieldmaps were calculated using four methods, 1) “ideal” – separate fieldmaps at each of the four locations/orientations, this represents the best estimate of the underlying off-resonance pattern 2) “static” – use the fieldmap at first position for all subsequent positions, (currently used in most fMRI studies) 3) “motion corrected” – use estimated motion parameters to rotate and translate the static fieldmap to the current orientation of the phantom, 4) “dynamic” – use joint estimation to obtain dynamic fieldmaps. We compared the images reconstructed using CP reconstruction method and iterative reconstruction method using - static, rotated, ideal and dynamic fieldmaps. Dynamic fieldmaps were used with the iterative reconstruction only. The reconstructed images at the four positions were registered to the initial position, using MCFLIRT [7], and the Normalized Root Mean Square Error (NRMSE) of the motion corrected images and reference image (image position 1) was compared across the various image reconstruction and fieldmap estimation methods.

Results & Discussion:

Fieldmaps: Row-1 (R1) in fig1 shows the off-resonance patterns or fieldmaps (FM) at four different orientations of the phantom. These patterns differ significantly with changing phantom orientation.

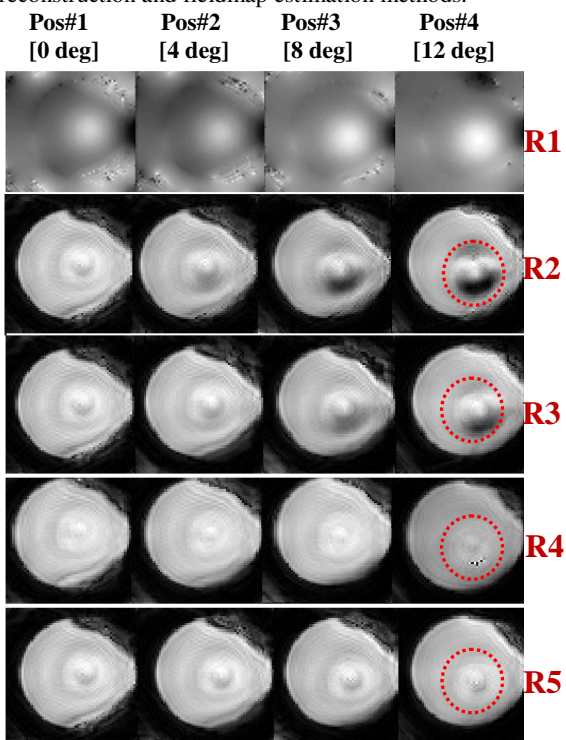
Images: image artifacts due to changing off-resonance patterns are most prominent at position 4 for images in R2 (static FM) & R3 (motion corrected FM). At this position, the phantom is “furthest” from its original orientation and, as can be seen in R1, the off-resonance patterns differ maximally from original pattern. Note, images in R4 (dynamic FM) & R5 (ideal FM), the artifacts in images at position 4 are suppressed as the dynamic and ideal FMs capture the “changed” off-resonance patterns more accurately than static and motion corrected FM at this orientation. In general, the effectiveness of static FM based correction (R2-fig1) reduces as the phantom orientation moves further from its original position. On motion correcting the static FM (R3-fig1), the image artifact seems to improve but, not completely. The jointly estimated dynamic FM is best able to correct for the position dependent artifacts (see R4-fig1) and the images are similar to the ones corrected using the ideal FM (R5-fig1).

Motion Correction: Table 1 summarizes the effect of the above listed off-resonance correction methods on the quality of image registration. CP gridding and iteratively reconstructed images of the phantom at position #4 were registered to the images at position #1, (reference) and the NRMSE between registered and reference was used as a measure of effectiveness of motion correction, lower NRMSE suggesting a more accurate registration. For ideal and dynamically updated FM, the NRMSE is the lowest and, equal to each other suggesting that these methods more effectively reduced dynamic off-resonance artifacts and improved image registration. As expected, static FM corrected image perform worse both, in iterative and CP case followed by images reconstructed motion corrected fieldmaps while, “ideal” FM performed the best.

FIGURE 1: R1 - fieldmaps (FM) at 4 positions, R2 – iterative recon. w/ static FM, R3 – iterative recon. w/motion corrected FM, R4 – iterative recon. w/dynamically updated FM, R5 – iterative recon. w/ideal FM.

References: [1]-MRM, 1996. 35(3):p346-55, [2]-Neuroimage, 2001. 14(3): p. 709-22, [3]-MRM, 1997. 38(1): p.151-60, [4]-IEEE TMI, 1991. 10(4): p. 629-637, [5]- IEEE Trans Med Imaging, 2003. 22(2): p. 178-88, [6]-MRM, 2004. 51(6): p. 1194-204, [7]-

<http://www.fmrib.ox.ac.uk/fsl/> **Acknowledgement:** This work is supported by NIH Grant EB002683



| NRMSE | STATIC | MOT. COR | DYN | IDEAL |
|-------|--------|----------|-----|-------|
| CP | 23% | 22% | | 20% |
| ITER | 21% | 20% | 16% | 16% |

TABLE 1: NRMSE after motion correction for the phantom images in pos #4, ref image = pos #1.